Available online at www.sciencedirect.com

SCIENCE DIRECT®

Mathematical Biosciences 188 (2004) 81–97

Mathematical Biosciences

www.elsevier.com/locate/mbs

Stochastic resonance and synchronization in the crayfish caudal photoreceptor

Sonya Bahar [a,*], Frank Moss [b]

[a] *Department of Neurological Surgery, Weill-Cornell Medical College, 525 East 68th Street, Box #99,*
New York Presbyterian Hospital, New York, NY 10021, USA
[b] *Center for Neurodynamics, University of Missouri at St. Louis, 8001 Natural Bridge Road, St. Louis, MO 63121, USA*

Received 17 December 2002; received in revised form 29 August 2003; accepted 16 September 2003

Abstract

Stochastic resonance is the process by which noise added to a weak external stimulus can enhance encoding efficiency in the sensory periphery and thence in the central nervous system. Stochastic synchronization is the process by which noisy phase synchronization of two periodic (or aperiodic) signals can occur. Together with a brief review of both concepts, we illustrate their applications to the encoding of weak external hydrodynamic signals in the mechanosensory system of the crayfish.

Keywords: Stochastic synchronization; Stochastic resonance; Crayfish photoreceptor; Crayfish mechanoreceptor; Sensory coding

---

1. Introduction to stochastic resonance

Stochastic resonance (SR) is an ubiquitous phenomenon found in both natural and man-made systems spanning a range of disciplines from physics and engineering to biology and medical science [2,27,48,49,51,79]. Only three ingredients are necessary for SR: a threshold, a subthreshold signal, and noise. Since these ingredients abound in nature and in man-made devices, it is no wonder that SR is widely found. SR was originally thought to be exclusively a dynamical phenomenon [27,33,34] and was frequently modeled as a particle moving in a one-dimensional, bistable potential under the influence of a weak periodic modulation and noise, for example,

---

[*] Corresponding author. Tel.: +1-212 746 5535; fax: +1-212 746 5592.
E-mail address: ssb2001@med.cornell.edu (S. Bahar).

doi:10.1016/j.mbs.2003.09.004

$$U(x) = -\frac{x^2}{2} + \frac{x^4}{4} + x[B\cos(\omega t + \phi) + \xi(t)], \tag{1.1}$$

where the signal amplitude B is smaller than the barrier height: $B < \frac{1}{4}$, and $\xi(t)$ is the noise usually assumed to be Gaussian and delta-correlated. The motion is then given by a Langevin equation,

$$\dot{x} = x - x^3 + B\cos(\omega t + \phi) + \xi(t). \tag{1.2}$$

This motion, $x(t)$, is a switching between potential wells (at $\langle x_0 \rangle = \pm 1$) marked by barrier crossings at random times, albeit times that correlate with the weak signal. (Note that we write $\langle x_0 \rangle = \pm 1$ rather than $x_0 = \pm 1$. This is because the particle on average spends equal time in each well. When there is noise, the well is tipped randomly back and forth, and the location of the exact minimum varies slightly around +1 or around −1.) The result resembles a random telegraph signal with noise. The barrier crossings were first identified with sensory neural encoding by comparison with experimental data (on monkey auditory system and cat visual cortex with weak periodic stimulations). These observations provided the first theoretical understanding of the phenomenon of 'skipping' frequently observed in sensory systems subject to weak periodic stimuli and internal neural noise [38].

The signature of SR is an inverted U-shaped curve of some information measure versus the noise intensity. That is, for a given barrier height and signal amplitude, there is an optimal noise intensity that maximizes the information in the response time course, $x(t)$. The simplest and most commonly used measure is simply the signal-to-noise ratio (SNR) of the response. The SNR is usually obtained from the power spectrum of $x(t)$. Thus the SNR is a maximum when the noise is at the optimal intensity. A complete statistical solution of Eq. (2) is only available in approximation, since it involves a time dependent Fokker–Planck equation (see for example [66]). An early approximate solution has been obtained within the framework of linear response theory [33,34].

An entirely new insight emerged from the development of the theory of non-dynamical SR by Laszlo Kish and colleagues in 1995 [29,51]. In this view, SR is exclusively a statistical phenomenon with the same three necessary ingredients: threshold, signal and noise. Fig. 1(A) illustrates the statistical view. The paradigm is that no information regarding the subthreshold signal (sine wave) can be transmitted if there is no crossing of the threshold, marked by the solid line lying a distance Δ_0 above the mean of the signal. Without noise, indicated by the irregular gray tracing, there are no threshold crossings and hence no information. With noise added to the signal (in this case Gaussian and band limited), threshold crossings appear. The upper trace shows the temporal sequence of positive threshold crossings marked by a train of pulses of standard shape. If we imagine all this to be taking place inside a black box, then the only information we have about the subthreshold signal is contained in the train of marker pulses (the box output).

This train contains a surprising amount of information about the subthreshold signal. For example, the power spectrum of the pulse train, shown in Fig. 1(B), shows sharp peaks at the fundamental signal frequency, f_0, and its second harmonic. We wish to obtain the area enclosed by the peak at f_0 above the noise background and the area in a 1 Hz bandwidth bounded at the top by the noise background. The SNR is defined as the ratio of the former to the latter. Changing

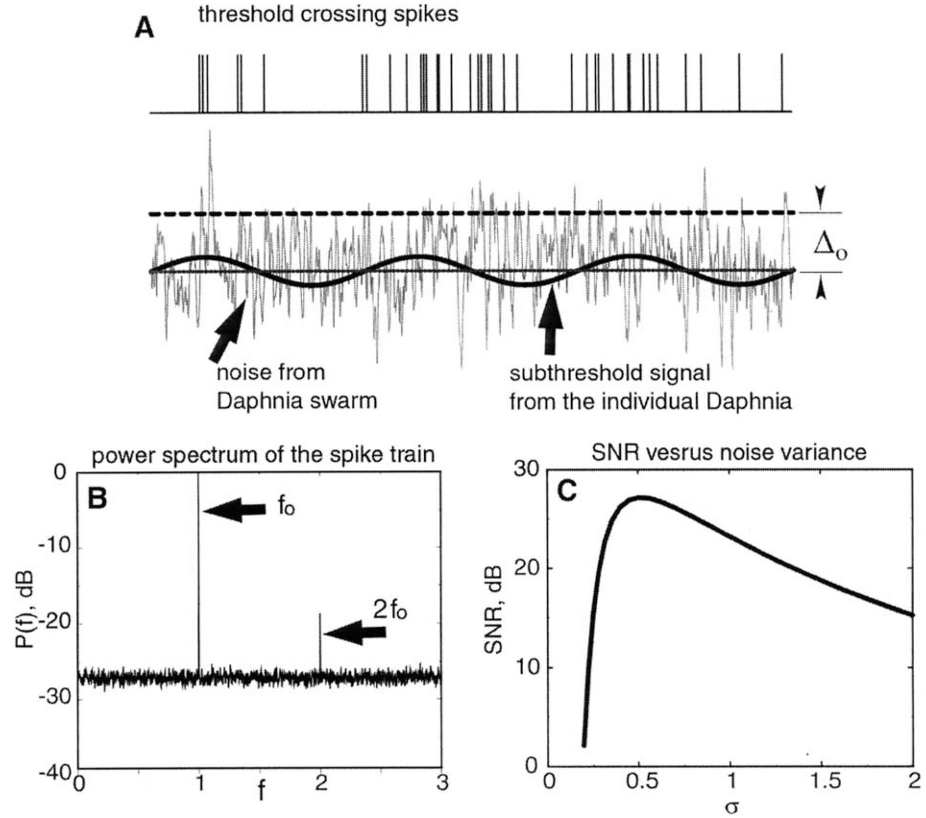

Fig. 1. Scheme of the theory of non-dynamical or threshold stochastic resonance. (A) Subthreshold signal (sine wave), threshold (dashed line) at Δ_0 above the mean of the signal and added noise (shaded irregular trace). This is a simulation in which the external, environmental noise emanates from a swarm of *Daphnia*, a freshwater zooplankton. See [25,26]. The spike train that marks the positive going threshold crossings of the signal plus the noise is shown above. (B) Power spectrum of the spike train. Each spike is converted to a delta function and the time average power spectrum is computed. Note the strong 2nd harmonic that is a distinctive feature of threshold SR and shows up in experiments as well. (C) The signal-to-noise ratio (SNR) computed from the power spectra measured at various noise intensities. The SNR passes through a maximum at an optimal noise intensity, the signature of SR.

the intensity of the noise added to the signal, as measured by its standard deviation, σ, results in a different SNR. As shown in Fig. 1(C) the SNR is small for small noise and again small for very large noise. There is thus an optimal noise intensity that maximizes the SNR. This inverted U-shaped curve is the signature of SR.

One can think of the noise as a sampling function. If the intensity is too small, there are too few samples per cycle of the signal. If too large the output is randomized at the expense of information regarding the signal. In both cases the information content in the train of marker pulses suffers. In our case, however, the noise is a one-bit sampler. No information on the amplitude of the signal is sampled, only the threshold crossing time. Early studies on random sampling and the reconstruction of power spectra were published by [8,41,57].

2. Theory of non-dynamical SR

Our task is to calculate the SNR from the set-up shown in Fig. 1. Here we will only outline the procedure as it has been expounded in detail elsewhere [51]. The essential element is to find the mean threshold crossing rate, $\langle v\rangle$. This quantity has been obtained for Gaussian band limited noise [65],

$$\langle v\rangle = \exp\left(-\frac{\Delta^2}{2\sigma^2}\right)\left[\frac{\int_0^\infty f^2 S(f)\,\mathrm{d}f}{\int_0^\infty S(f)\,\mathrm{d}f}\right]^{1/2}, \tag{2.1}$$

where Δ is the threshold, σ is the standard deviation of the (Gaussian) noise and $S(f)$ is its power spectrum. We can simplify by assuming that $S(f)$ is a rectangular function with upper cut-off frequency f_n, whence,

$$\langle v\rangle = \frac{f_n}{\sqrt{3}}\exp\left(-\frac{\Delta^2}{2\sigma^2}\right). \tag{2.2}$$

We now let the threshold become a slow function of time with Δ_0 its mean,

$$\Delta(t) \to \Delta_0 + B\sin(2\pi f_0 t), \tag{2.3}$$

whence, $\langle v\rangle \to \langle v\rangle(t)$ also becomes a slow function of time. Here 'slow' means that $f_0 \ll \langle v\rangle$, so that the signal is adequately sampled by the noise during a cycle. This is in the spirit of rate coding in neuroscience. The mean threshold crossing rate, $\langle v\rangle(t)$, encodes the instantaneous amplitude of the signal, $B\sin(2\pi f_0 t)$ in the spike train shown in Fig. 1(A).

Supposing that the amplitude of the marker pulses is A and their width τ, then the mean amplitude of the spike train is $\langle V\rangle = A\tau\langle v\rangle(t)$. The power spectra of the spike train and noise are then

$$\begin{aligned} S_s(f) &= \left(\frac{A^2\tau^2 f_0^2}{3}\right)\left[\left(\frac{\Delta_0 B}{\sigma^2}\right)^2\delta(f_0) + \left(\frac{B^2}{4\sigma^2}\right)^2\delta(2f_0)\right]\exp\left(-\frac{\Delta_0^2}{\sigma^2}\right), \\ S_n(f) &= \frac{1}{2}A^2\tau^2\langle v\rangle, \end{aligned} \tag{2.4}$$

Approximations used in deriving Eq. (2.4) are $\tau \ll \langle v\rangle^{-1}$, $B/\sigma \ll \Delta_0$, and we have dropped all harmonics higher than the second. For details see [51]. The SNR in units of decibels (dB) is then

$$\mathrm{SNR} = 10\log_{10}\left[\frac{2f_0\Delta_0^2 B^2}{\sqrt{3}\sigma^4}\right]\exp\left(-\frac{\Delta_0^2}{2\sigma^2}\right), \tag{2.5}$$

and this function has been used to plot the graph in Fig. 1(C). It is the combination of the inverse σ^4 in the prefactor and the inverse σ^2 in the exponent that result in the maximum at the optimal noise intensity.

In this process, the addition of the noise is essential to the detection of the subthreshold signal and for the transmission of information about the signal through the system. Moreover, we note that the system outlined here and in Fig. 1 represents the simplest model for a single sensory neuron [28,35,43], and according to this view noise plays a constructive role in its operation. Indeed, noise has always played a role in the neurosciences [1,45]. An informative and interesting review has been provided by Segundo et al. [70]. Early studies on the effects of noise on sensory detection and processing in amphibians were published by Narins and colleagues [89,90].

3. Some experiments on SR in sensory biology

SR was demonstrated experimentally first in an electronic circuit [24] and later in a ring laser [42]. It was observed in sensory biology using the hydrodynamically sensitive mechanoreceptive system of the crayfish [19] and soon after in the cercal system of the cricket [36]. Both animals belong to the same phylum and thus have similar neural architectures. The crayfish *Procambarus clarkii* is shown in Fig. 2 (upper panel) together with a diagram of its peripheral mechanosensory

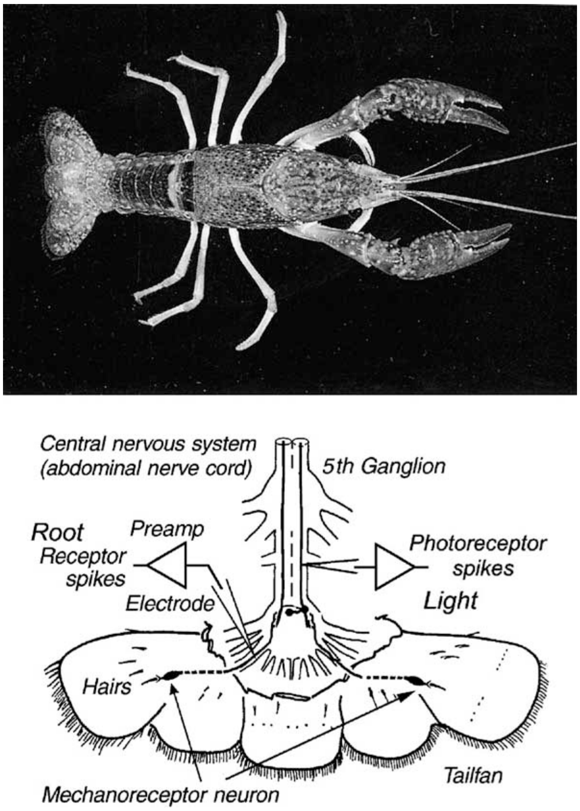

Fig. 2. A red swamp crayfish, *Procambarus clarkii* (upper panel), the species used in the present experiments. A schematic diagram of the crayfish mechanoreceptive system showing hairs, sensory afferents (the root receptors) that synapse on the two caudal photoreceptor (CPR) neurons embedded in the 6th, or caudal, ganglion. The lower electrode and amplifier record root responses while the upper electrode and amplifier record responses of the CPR. Light impinging on sensitive areas (solid circles, approximate locations) mediated the transduction of hydrodynamic signals from the root.

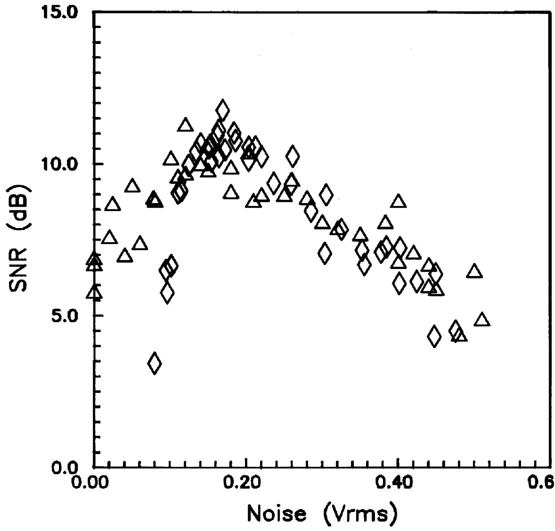

Fig. 3. SR data from recordings at the sensory afferents (root): crayfish data (open triangles); simulation by a FitzHugh–Nagumo neuron model (open diamonds). The horizontal axis represents the rms voltage input to an electromechanical motion transducer that moves the tailfan preparation through the fluid. The actual displacements ranged from 0 to 250 nm.

system (lower panel). The tailfan and 5th and 6th ganglia were mounted in an apparatus for producing motions relative to an immersion fluid [20,86]. The motions were calibrated with a laser Doppler vibrometer. Both periodic and random motions in the range 10–500 nm were produced. Recordings were made of the sensory neural spike trains from the root receptors as shown in the lower panel of Fig. 2. Spike trains similar to the simulated ones of Fig. 1 were analyzed and the SNRs computed. Example results are shown by the triangles in Fig. 3. The diamonds are the result of a simulation of the crayfish sensory neuron using a FitzHugh–Nagumo model [50]. These data show the classical signature: an inverted U-shaped curve of SNR versus noise intensity.

4. SR in human and animal perception

The crayfish and cricket experiments have been complemented by many demonstrations of SR or stochastic resonance-like phenomena in various biological preparations including at the molecular [7,9], cellular [3] and neural [4,5,11,12,15,39,61] levels. Applications to human sensory neurons include proprioceptive neurons [17] and cochlear implants [31,47]. However, these demonstrations of SR in peripheral neurons beg the question: can the animal perceive and make use of this enhanced information? In order to address this question behavioral experiments with animals and/or human psychophysics experiments are necessary. But before exploring this, a brief digression on thresholds is called for.

The threshold represented by the dashed line in Fig. 1(A) is a 'hard' threshold. The system responds with a marker pulse (a spike) only when the threshold is crossed with probability one.

But SR also obtains with a class of 'soft' thresholds that can be statistical functions that describe the threshold crossing probability. They are typically steeply rising functions of stimulus amplitude and can represent *perceptive* thresholds in animals and humans. The conditions that can give rise to SR in such systems have been analyzed by Ward et al. [83].

Indeed, SR has been demonstrated in animal behavior [30,69] engendering the term 'behavioral SR' [25,26]. It has also been demonstrated in human perception [16,71,72,80,82] and cognitive tasks [62,76]. See also a discussion of SR in the excellent book on dynamical cognition [81].

Soft thresholds also abound in medical science so it is not surprising that SR has also found applications in electromyography [13,14], rehabilitation [37,75], respiration [74], the cardiovascular and baro-reflexive systems [32,87] and brain function [40,46,88].

5. Introduction to stochastic synchronization

Stochastic synchronization (SS) is a general topic that addresses the phenomenon of irregular phase locking between two noisy non-linear oscillators or between a non-linear oscillator and an external driving force. In neuroscience it is closely related to encoding schemes that depend on the timing precision of neural spikes [60]. It is also closely related to SR [53] since the barrier crossings in a driven oscillator with a bistable potential given, for example, by Eq. (1.1) will to some extent be in phase synchronization with the weak driving signal, $B\cos(\omega t)$. The Langevin Equation in this case is

$$\ddot{x} - \gamma\dot{x} + \omega_0^2 x = x - x^3 + B\cos(\omega t) + \xi(t), \tag{5.1}$$

where γ is the damping. What is phase synchronization? An excellent book treats the general subject [63]. When an oscillator such as the one described by Eq. (5.1) is driven by a periodic (or non-periodic) function, the phase difference between the oscillator response and the driving function tends to a constant. This is called 'phase locking' and it must persist over a finite range of system parameters. Phase synchronization can be of order $n:m$ for which n cycles of the drive ($\psi(t)$) match up in final phase with m cycles of the oscillator ($\phi(t)$), and this phase difference, $\Phi_{n,m}(t)$, will remain constant in time. The following serves as a definition of SS:

$$\begin{aligned} \Phi_{n,m} &= |n\phi(t) - m\psi(t)| < \text{const.}, \\ \omega &= \langle\dot{\phi}\rangle = \frac{m}{n}\omega_0 = \frac{m}{n}\langle\dot{\psi}\rangle, \end{aligned} \tag{5.2}$$

and the angular brackets indicate time averages of sufficient length to establish the indicated quantities to within some determined statistical confidence level.

Of course, if there is noise in either the oscillator or the drive or both, the phase tends to lock for some (random) time periods, called epochs, interspersed with periods when the phase difference drifts [54,67,68]. The phase difference, $\Phi_{n,m}$, can be represented as diffusing in a tilted periodic potential and can be described by an effective diffusion constant [73]:

$$\langle\Phi_{n,m}^2(t)\rangle - \langle\Phi_{n,m}(t)\rangle^2 \propto D_{\mathrm{eff}_{n,m}} t. \tag{5.3}$$

The statistical quality of the synchronization is represented by the probability density of the phase difference, $P(\Phi_{n,m})$. A single factor, the synchronization index, can be defined as the first Fourier mode of this density:

$$\gamma_{n,m}^2 = \langle \cos(\Phi_{n,m}(t)) \rangle^2 + \langle \sin(\Phi_{n,m}(t)) \rangle^2. \tag{5.4}$$

This factor varies from 0 (no synchronization) to 1.0 (perfect synchronization, meaning no phase diffusion).

But our special interest here is to describe the case of a noisy *neural* oscillator being driven by an (external) periodic forcing function. The response of the neural oscillator is a spike train, and we must define the phase of the spikes relative to the phase of the forcing function. SS between such a neural oscillator and an external forcing was observed for the paddlefish electroreceptor system [55,56], and the theory described in [56,63,68]. If a neural spike occurs at a time t_k compared with the upward zero crossing times of the driving function, τ_i, then the phase difference is

$$\phi(t_k) = 2\pi \frac{t_k - \tau_i}{\tau_{i+1} - \tau_i}, \tag{5.5}$$

where $\tau_i < t_k < \tau_{i+1}$. This (discrete) phase difference can have values $0 < \phi < 2\pi$. There is also a definition of the continuous phase difference which spans the range $-\infty < \phi < \infty$:

$$\phi(t) = 2\pi \frac{t - \tau_i}{\tau_{i+1} - \tau_i} + 2\pi i. \tag{5.6}$$

And in this case, also, the neuron may fire m times during n cycles. The phase locking condition is defined as before, but now it applies only during the epochs of phase locking: $|n\phi(t) - m\phi_{\text{stim}}(t)| < \text{const.}$, where $\phi_{\text{stim}} = 2\pi f_0 t$ is the phase of the drive (or stimulus). The phase difference between the spike train and the drive is then

$$\Phi_{n,m}(t) = \left[2\pi \frac{t - \tau_i}{\tau_{i+1} - \tau_i} + 2\pi i \right] n - 2\pi m f_0 t. \tag{5.7}$$

Again, the synchronization index given in Eq. (5.4) gives a statistical measure of the strength of the synchronization.

In the following section we will show SS in the crayfish caudal photoreceptor neuron and describe its relation to SR.

6. SS in the crayfish caudal photoreceptor neurons

A simplified wiring diagram of the crayfish mechanoreceptive system was shown in Fig. 1(B). We focus on the upper recording amplifier attached to one of the caudal photoreceptor neurons (CPR). Periodic, hydrodynamic stimuli are applied to the array of hairs on the tailfan with a motion transducer. The motion of the liquid saline medium relative to the hairs was calibrated with a laser Doppler vibrometer. Each hair is innervated by two sensory neurons that converge on the interneurons of the 6th ganglion [77,78]. Two of these interneurons – the CPRs – are photosensitive. Our experiment could be carried out in dark conditions such that the light intensity

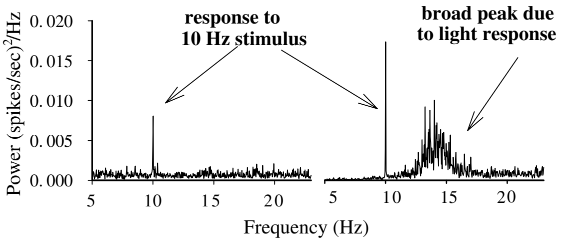

Fig. 4. Power spectra of the CPR response to a 9 μm, 10.5 Hz, sinusoidal hydrodynamic signal in dark conditions (<5 nW/mm^2) (trace at left) and in the light (22 μW/mm^2) (trace at right). The peaks at 10.5 Hz are the signatures of the stimulus. The peaks at around 17 Hz are due to the internal CPR oscillator.

falling on the preparation was smaller than 5 nW/mm^2. Alternatively, light with an incandescent spectrum was applied by way of a fiber optic cable to the light sensitive regions near the CPR neurons just under the carapace on the 6th ganglion [85]. Steady dim light falling on the sensitive regions mediates the transduction efficiency of the hydrodynamic motion into neural spike trains in the CPR. Indeed, dim light compared to dark conditions has been shown to result in better than one order-of-magnitude in the SNR measured at the CPR [61]. This is shown by the two power spectra of CPR spike train recordings displayed in Fig. 4, where the heavy dark trace applies to dark conditions and the lighter trace to a light intensity of 22 μW/mm^2 (approximately comparable to dim room light). In both cases the amplitude of the hydrodynamic stimulus was 9.0 μm at a frequency of 10.5 Hz. The sharp peaks at 10.5 Hz show the signatures of the periodic stimulus. The SNR of the light trace (transduction mediated by the light) is approximately one order of magnitude larger than the one for the heavy dark trace (dark conditions).

Significantly, the CPRs are oscillators, albeit noisy ones. The firing rate of this oscillator is modulated by light [85]. In the dark, the oscillator fires around 5–7 Hz, but is so obscured by noisy hydrodynamic input from the mechanorecptors that it may appear almost Poisson-like. Thus the heavy trace in Fig. 4, minus the peak at 10.5 Hz, is nearly flat. In the light, the oscillator, now firing much faster can become a more dominant part of the signal, though it is still extremely noisy (see the broad peak around 17 Hz in the lighter trace in Fig. 4).

The calculation of the phase difference between the oscillator and the drive, and the computation of the synchronization index, Eq. (5.4), are extremely powerful tools for exposing the nature of oscillatory phenomena even when they are largely obscured by noise, as is so often the case in the messy world of biological systems. In Fig. 5, we show two synchrograms (left panels) and their associated probability densities of phase differences (right panels) measured under dark conditions. The synchrograms are time records of the instantaneous phase differences (Eq. (5.5)) between the stimulus function and the spike elicited at the CPR. In this case only one spike (on average) is elicited per single stimulus cycle, so that the order is 1:1. The upper panel is for a stimulus frequency of 10.5 Hz, amplitude 6 μm. It shows well-synchronized behavior as indicated by the dark density of phases at around $\Phi \approx 1.7$ radians on the synchrogram and the corresponding pronounced peak in the density. We recall that the synchronization index, γ, as defined by Eq. (5.4) is the normalized first Fourier mode of the density. Thus it will be strongly sensitive to the presence of such peaks. In contrast, the lower panel indicates the result for the same conditions

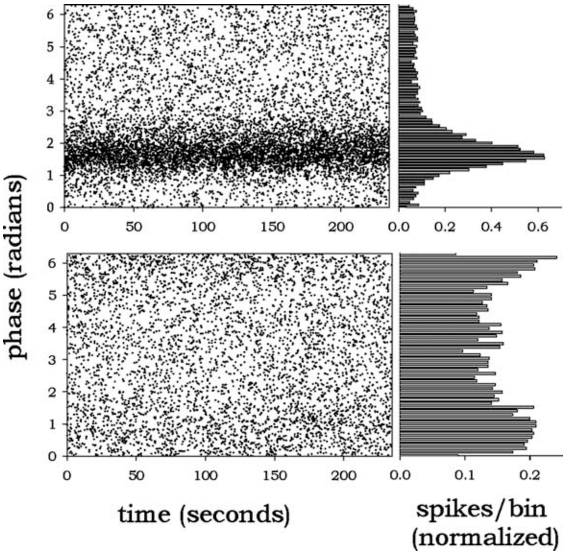

Fig. 5. Synchrograms (left panels) and probability densities of phase differences (right panels) for the CPR forced at 6 μm in dark conditions. Upper panels, 10.5 Hz forcing frequency, lower panels, 20 Hz forcing frequency. The upper panels indicate 1:1 synchronization.

except now the forcing frequency is 20 Hz, which is near the outer limit of the CPR's frequency range. Here, the response is much noisier than in the top panels, and no clear peak is evident in the phase difference histogram at the bottom right.

A distinct hallmark of stochastic synchronization is the (statistical) entrainment between the oscillator and the drive over a *range* of frequencies. Fig. 6 shows five examples of synchronization indices of differing orders measured as functions of the forcing frequency. Note the meaning of the subscripts on the indices $\gamma_{n,m}$. The uppermost trace is $\gamma_{1,2}$ with 2 spikes (on average) per 1 stimulus cycle. Note that this index peaks at the relatively low forcing frequency approximately 2 Hz. The subsequent traces show sequential lockings for larger forcing frequencies. Note the vertical scales. As expected, the fundamental locking $\gamma_{1,1}$ is the largest, indicating that at this forcing frequency the phase locking epochs persist on average for longer times. Lockings up to the 4th order are shown; in fact, the progressive sequence of maximum synchronization indices shows the system passing through a series of Arnol'd tongues!

So what is the effect of light on the CPR? Evidently it is to push the CPR oscillators toward larger natural frequencies. This is indicated by the sequence of lockings shown in Fig. 7 for orders 1:2 < 1:1 < 2:1. The indices measured under dark conditions are shown by the solid circles, and those measured in the light (22 μW/mm^2) are indicated by the open squares. The pushing effect is largest for the subharmonic 1:2 locking where the maximum or the index is pushed from about 3 Hz (dark) to about 10 Hz (light). The fundamental 1:1 locking and the 2:1 locking also show significant increases of the natural frequencies in the light. To our knowledge, there is no reason why higher-order lockings (such as 3:2, 5:2) are not, in principle, possible in this system. Due to the noisiness of the system, however, observation of these lockings in practice is highly unlikely.

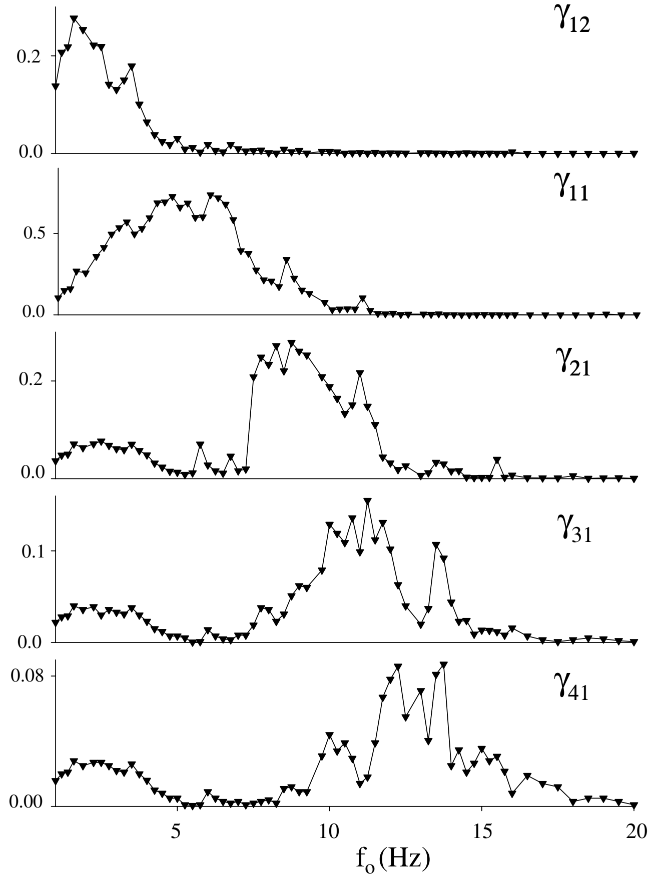

Fig. 6. Synchronization indices showing sequential phase lockings commencing with the subharmonic order, 1:2, and proceeding through higher orders to 4:1.

7. SS and SR in the crayfish caudal photoreceptor

As discussed in Section 5 above, SR and SS are closely related. This can be demonstrated in the crayfish CPR by simultaneously measuring the power spectra (and hence the SNR) and the synchronization indices. In classical SR, the control parameter is the noise intensity that is added to the weak signal to enhance threshold crossings and hence detectability as shown in Fig. 1. In the crayfish CPR however, the noise is internal. Indeed it is internal to the entire 6th ganglion, since the interneurons are barraged by random noise arriving from the myriad sensory afferents [19,59]. In the CPRs we speculate that the light intensity is related to this internal noise. If true, light can enhance signal transduction by the mechanism of SR.

Moreover, if SR and SS are closely related there should be a relation between the synchronization index and the SNR [54]. Our simultaneous measurements of the power spectra and the 1:1 synchronization indices have revealed such a relation as shown in Fig. 8. The solid circles represent the SNR and the open circles represent the 1:1 index for a range of light levels. The two sets

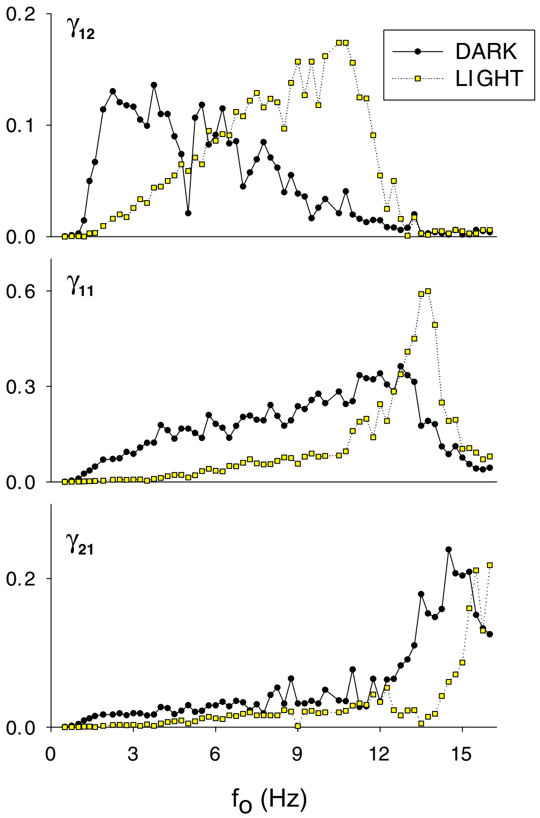

Fig. 7. Effects of light on the synchronization indices at three orders for dark conditions (solid circles) (<5 nW/mm^2) and in the light (open squares) (22 μW/mm^2). Note that light pushes the indices toward higher frequencies.

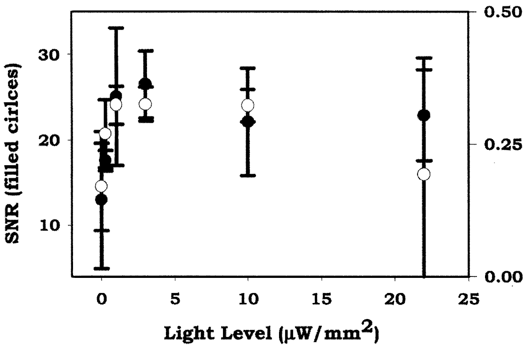

Fig. 8. SR and SS in the caudal photoreceptor. SNR (solid circles) and synchronization index (open circles) versus light intensity, where light intensity is a surrogate for noise intensity.

of data clearly follow the same trends, both showing maxima at approximately the same optimal light (possibly noise) intensity. To our knowledge this experiment, first reported in Bahar et al. [4], constitutes the first experimental demonstration of this relation, first predicted by Neiman et al. [54], in a biological setting.

8. Discussion and conclusions

It is as yet unknown what, if anything, the phenomenon of phase locking may mean to the animal and if it helps the crayfish avoid predation. However, the evidence is suggestive. The tail-beat and fin-beat frequencies of many crayfish predators [6,10,21–23,84] are within the photoreceptor/mechanoreceptor's sensitivity range of 2–18 Hz. If the otherwise random (i.e. unsynchronized) responses of many modalities are prompted to respond in phase synchrony by the predator's approach, then these responses arrive at centers in the higher nervous system within smaller time windows. They thus result in larger instantaneous responses by summing modalities, a process that is thought to form the basis of much sensory detection. However, this is not what happens in the crayfish. The external stimulus can only be perceived by the animal through the firing of the photoreceptor. This means that the crayfish itself has no way to compare its CPR firing with the stimulus. In other words, calculations of synchronization indices are inaccessible to the animal's own nervous system. It is possible that some interpretation of the SNR from the power spectrum, however, which is contained within the time series of spikes fired by the photoreceptor, can be deciphered by upstream neurons receiving input from the CPR.

And why the light sensitivity? Crayfish are largely nocturnal creatures. But they do often venture outside their burrows in daylight to forage for food. The light induced upward frequency push at least for the 1:1 locking is accompanied by a much larger synchronization index. Thus the spike timing precision (spikes per unit time arriving in a narrower time window) is increased in the light. In this way, the crayfish may achieve a heightened awareness of hydrodynamic disturbances that signal danger when foraging in the daylight and subject to the depredations of visual predators. A similar speculation was first advanced in [61].

The crayfish is possessed of an exquisitely sensitive mechanoreceptive system, being capable of detecting water motions as small as a few tens of Ångstroms [19,64]. It thus joins other animals with notably sensitive receptors, for example seismic waves [52] or electric fields [69]. Moreover it is a primitive system dating from at least 225 million years ago [44,58]. The crayfish uses its caudal mechanoreceptive system for predator avoidance and it is evidently highly effective, the animal having spread over the whole globe (except Africa and, presently, Antarctica) in at least 590 species [18]. But the system is also inherently noisy [19,59]. How can such a primitive and noisy system achieve such evolutionary success? We have not answered this question in this paper, but hopefully we have introduced sensory biologists and biophysicists to some suggestive processes associated with the animal's stimulus-detecting and information-processing capabilities.

We have reviewed the field of SR whereby noise can enhance both detectability and information processing capabilities. Perhaps SR plays a fundamental role in the evolution of such systems. As the science of noisy signal detection at the threshold of perception, SR may well have influenced the detailed way in which such receptors have evolved. We have discussed SR in the crayfish, outlining the development from the first observations of the phenomenon in biology to the present studies of the effects of light and higher processing within the 6th ganglion. Finally, we have outlined the relatively new field of SS by demonstrating its application to the crayfish sensory system.

We hope these studies will be suggestive and stimulating of further explorations of these two phenomena in other sensory systems.

Acknowledgements

We are grateful to Alexander Neiman, David Russell, Gabor Balázsi, Anke Ordemann and Lon Wilkens for numerous stimulating discussions. This work was supported by the Office of Naval Research, Physical Sciences Division. S.B. gratefully acknowledges support from a National Research Service Award from the NIH (NINDS). F.M. is grateful to the Alexander von Humboldt Foundation, Bonn, Germany for continuing support.

References

[1] W.R. Adey, Organization of brain tissue: Is the brain a noisy processor?, Int. J. Neurosci. 3 (1972) 271.

[2] V. Anishchenko, F. Moss, A. Neiman, L. Schimansky-Geier, Stochastic resonance: noise induced order, Sov. Phys. Usp. 42 (1) (1999) 7.

[3] R.D. Astumian, R.K. Adair, J.C. Weaver, Stochastic resonance at the single-cell level, Nature 388 (1997) 632.

[4] S. Bahar, A. Neiman, L.A. Wilkens, F. Moss, Phase synchronization and stochastic resonance effects in the crayfish caudal photoreceptor, Phys. Rev. E (Rapid Comm.) 65 (2002) 050901.

[5] S. Bahar, F. Moss, The nonlinear dynamics of the crayfish mechanosensory system, Int. J. Bifurc. Chaos 13 (8) (2003) 2013.

[6] R. Bainbridge, The speed of swimming of fish as related to size and to the frequency and amplitude of the tail beat, J. Exp. Biol. 35 (1958) 109.

[7] F. Beck, B. Blasius, U. Lüttge, R. Neff, U. Rascher, Stochastic noise interferes coherently with a model biological clock and produces specific dynamic behaviour, Proc. Roy. Soc. Lond. B 268 (2001) 1307.

[8] F.J. Beutler, Alias-free randomly timed sampling of stochastic processes, IEEE Trans. Info. Theory 16 (1970) 147.

[9] S.M. Bezrukov, I. Vodyanoy, Noise-induced enhancement of signal transduction across voltage-dependent ion channels, Nature 378 (1995) 362.

[10] H. Bleckmann, T. Breithaupt, R. Blickhan, J. Tautz, The time course and frequency content of hydrodynamic events caused by moving fish, frogs and crustaceans, J. Comp. Physiol. A 168 (1991) 749.

[11] H.A. Braun, H. Wissing, K. Schäfer, M.C. Hirsch, Oscillation and noise determine signal transduction in shark multimodal sensory cells, Nature 367 (1994) 270.

[12] D.R. Chialvo, A.V. Apkarian, Modulated noisy biological dynamics: three examples, J. Stat. Phys. 70 (1993) 375.

[13] F.Y. Chiou-Tan, K. Magee, L. Robinson, M. Nelson, S. Tuel, T. Krouskop, F. Moss, Enhancement of subthreshold sensory nerve action potentials during muscle tension mediated noise, Int. J. Bifurc. Chaos 6 (1996) 1389.

[14] T.-Y. Chuang, L.R. Robinson, M.R. Nelson, F. Moss, F. Chiou-Tan, Effect of isometric contraction on threshold somatosensory evoked potentials, Am. Phys. Med. Rehabil. 78 (1999) 2.

[15] J.J. Collins, T.T. Imhoff, P. Grigg, Noise-enhanced information transmission in rat SA1 cutaneous mechanoreceptors via aperiodic stochastic resonance, J. Neurophysiol. 76 (1996) 642.

[16] J.J. Collins, T.T. Imhoff, P. Grigg, Noise-enhanced tactile sensation, Nature 383 (1996) 770.

[17] P. Cordo, T. Inglis, S. Verschueren, J. Collins, D. Merfeld, S. Rosenblum, S. Buckley, F. Moss, Noise in human muscle spindles, Nature 383 (1996) 769.

[18] K.A. Crandall, J.W. Fetzner, The Crayfish Home Page, 2002. http://zoology.byu.edu/crandall_lab/crayfish/crayhome.htm.

[19] J.K. Douglass, L. Wilkens, E. Pantazelou, F. Moss, Noise enhancement of information transfer in crayfish mechanoreceptors by stochastic resonance, Nature 365 (1993) 337.

[20] J.K. Douglass, L.A. Wilkens, Directional selectivities of near-field filiform hair mechanoreceptors on the crayfish tailfan (Crustacea: Decapoda), J. Comp. Physiol. A 183 (1998) 23.

[21] E.G. Drucker, J.S. Jensen, Pectoral fin locomotion in the striped surfperch. I. Kinematic effects of swimming speed and body size, J. Exp. Biol. 199 (1996) 2235.

[22] E.G. Drucker, J.S. Jensen, Pectoral fin locomotion in the striped surfperch. II. Scaling swimming kinematics and performance at a gait transition, J. Exp. Biol. 199 (1996) 2243.

[23] D.J. Ellerby, J.D. Altringham, Spatial variation in fast muscle function of the rainbow trout *Oncorhynchus mykiss* during fast-starts and sprinting, J. Exp. Biol. 204 (2001) 2239.

[24] S. Fauve, F. Heslot, Stochastic resonance in a bistable system, Phys. Lett. 97A (1983) 5.

[25] J.A. Freund, J. Kienert, L. Schimansky-Geier, B. Beisner, A. Neiman, D. Russell, T. Yakusheva, F. Moss, Behavioral Stochastic Resonance: How a noisy army betrays its outpost, Phys. Rev. E 63 (2001) 031910.

[26] J. Freund, L. Schimansky-Geier, B. Beisner, A. Neiman, D. Russell, T. Yakusheva, F. Moss, Behavioral stochastic resonance: How the noise from a *Daphnia* swarm enhances individual prey capture by juvenile paddlefish, J. Theor. Biol. 214 (2002) 71.

[27] L. Gammaitoni, P. Hanggi, P. Jung, F. Marchesoni, Stochastic resonance, Rev. Mod. Phys. 70 (1998) 223.

[28] G.L. Gerstein, B. Mandelbrot, Random walk models for the spike activity of a single neuron, Biophys. J. 4 (1964) 41.

[29] Z. Gingl, L.B. Kiss, F. Moss, Non-dynamical stochastic resonance: theory and experiments with white and arbitrarily coloured noise, Europhys. Lett. 29 (1995) 191.

[30] P.E. Greenwood, L.M. Ward, D.F. Russell, A. Neiman, F. Moss, Stochastic resonance enhances the electrosensory information available to paddlefish for prey capture, Phys. Rev. Lett. 84 (2000) 4773.

[31] K.R. Henry, Noise improves transfer of near-threshold, phase locked activity of the cochlear nerve: evidence for stochastic resonance? J. Comp. Physiol. A 184 (1999) 577.

[32] I. Hidaka, D. Nozaki, Y. Yamamoto, Functional stochastic resonance in the human brain: noise induced sensitization of baroreflex system, Phys. Rev. Lett. 85 (17) (2000) 3740.

[33] P. Jung, Periodically driven stochastic systems, Phys. Rep. 234 (1993) 175.

[34] P. Jung, P. Hänggi, Stochastic nonlinear dynamics modulated by external periodic forces, Europhys. Lett. 8 (1989) 505.

[35] H. Landahl, W.S. McCulloch, W. Pitts, A statistical consequence of the logical calculus of nervous nets, Bull. Math. Biophys. 5 (1943) 135.

[36] J.E. Levin, J.P. Miller, Broadband neural encoding in the cricket cercal sensory system enhanced by stochastic resonance, Nature 380 (1996) 165.

[37] W. Liu, L.A. Lipsitz, M. Montero-Odasso, J. Bean, D.C. Kerrigan, J.J. Collins, Noise-enhanced vibrotactile sensitivity in older adults, patients with stroke and patients with diabetic neuropathy, Arch. Phys. Med. Rehabil. 83 (2002) 171.

[38] A. Longtin, A. Bulsara, F. Moss, Time-interval sequences in bistable systems and the noise-induced transmission of information by sensory neurons, Phys. Rev. Lett. 67 (1991) 656.

[39] E. Manjarrez, G. Rojas-Piloni, I. Méndez, L. Martínez, D. Vélez, D. Vázquez, A. Flores, Internal stochastic resonance in the coherence between spinal and cortical neuronal ensembles in the cat, Neurosci. Lett. 326 (2002) 93.

[40] E. Manjarrez, O. Diez-Martínez, I. Méndez, A. Flores, Stochastic resonance in human electroencephalographic activity elicited by mechanical tactile stimuli, Neurosci. Lett. 324 (2002) 213.

[41] E. Masry, Random sampling and reconstruction of spectra, Inform. Control 19 (1971) 275.

[42] B. McNamara, K. Wiesenfeld, R. Roy, Observation of stochastic resonance in a ring laser, Phys. Rev. Lett. 60 (1988) 2626.

[43] W.S. McCulloch, W. Pitts, The statistical organization of nervous activity, Biometrics 4 (1948) 91.

[44] G.L. Miller, S.R. Ash, The oldest freshwater decapod crustacean, from the Triassic of Arizona, Paleontology 31 (1988) 273.

[45] G.P. Moore, D.H. Perkel, J.P. Segundo, Statistical analysis and functional interpretation of neuronal spike data, Ann. Rev. Physiol. 28 (1966) 493.

[46] T. Mori, S. Kai, Noise-induced entrainment and stochastic resonance in human brain waves, Phys. Rev. Lett. 88 (2002) 218101.

[47] R. Morse, E. Evans, Enhancement of vowel coding for cochlear implants by addition of noise, Nature Med. 2 (1996) 928.

[48] F. Moss, Stochastic resonance: from the ice ages to the monkey's ear, in: G.H. Weiss (Ed.), Contemporary Problems in Statistical Physics, SIAM, Philadelphia, PA, 1994, p. 205.

[49] F. Moss, Stochastic resonance: looking forward, in: J. Walleczek (Ed.), Self-organized biological dynamics and nonlinear control, Cambridge University, Cambridge, UK, 2000, p. 236.

[50] F. Moss, J.K. Douglass, L. Wilkens, D. Pierson, E. Pantazelou, Stochastic resonance in an electronic FitzHugh–Nagumo Model, Ann. N.Y. Acad. Sci. 706 (1993) 26.

[51] F. Moss, D. Pierson, D. O'Gorman, Stochastic resonance: Tutorial and update, Int. J. Bifurc. Chaos 6 (1994) 1383.

[52] P.M. Narins, E.R. Lewis, The vertebrate ear as an exquisite seismic sensor, J. Acoust. Soc. Am. 76 (5) (1984) 1384.

[53] A. Neiman, A. Silchenko, V. Anishchenko, L. Schimansky-Geier, Stochastic resonance: noise-enhanced phase coherence, Phys. Rev. E 58 (1998) 7118.

[54] A. Neiman, L. Schimansky-Geier, F. Moss, B. Shulgin, J.J. Collins, Synchronization of noisy systems by stochastic signals, Phys. Rev. E 60 (1999) 284.

[55] A. Neiman, X. Pei, D. Russell, W. Wojtenek, L. Wilkens, F. Moss, H.A. Braun, M.T. Huber, K. Voigt, Synchronization of the noisy electrosensitive cells in the paddlefish, Phys. Rev. Lett. 82 (1999) 660.

[56] A.B. Neiman, D.F. Russell, X. Pei, W. Wojtenek, J. Twitty, E. Simonotto, B.A. Wettring, E. Wagner, L.A. Wilkens, F. Moss, Stochastic synchronization of electroreceptors in the paddlefish, Int. J. Bifurc. Chaos 10 (2000) 2499.

[57] H. Nyquist, Certain topics in telegraph transmission theory, AIEE Trans. 47 (1928) 617.

[58] A.S. Packard, Fossil crawfish from the tertiaries of Wyoming, Am. Natural. 14 (3) (1880) 222.

[59] E. Pantezelou, C. Dames, F. Moss, J. Douglass, L. Wilkens, Temperature dependence and the role of internal noise in signal transduction efficiency of crayfish mechanoreceptors, Int. J. Bifurc. Chaos 5 (1995) 101.

[60] X. Pei, L. Wilkens, F. Moss, Noise-induced spike timing precision from aperiodic stimuli in an array of Hodgkin–Huxley-type neurons, Phys. Rev. Lett. 77 (1996) 4679.

[61] X. Pei, L. Wilkens, F. Moss, Light enhances hydrodynamic signaling in the multimodal caudal photoreceptor interneurons of the crayfish, J. Neurophysiol. 76 (1996) 3002.

[62] M. Piana, M. Canfora, M. Riani, Role of noise in image processing by the human perceptive system, Phys. Rev. E 62 (2000) 1104.

[63] A.S. Pikovsky, M.G. Rosenblum, J. Kurths, Synchronization: A Universal Concept in Nonlinear Sciences, Cambridge University, Cambridge, 2001.

[64] M.R. Plummer, J. Tautz, J.J. Wine, Frequency coding of waterborne vibrations by abdominal mechanosensory neurons in the crayfish, *Procambarus clarkii*, J. Comp. Physiol. A Sens. Neural. Behav. Physiol. 158 (1986) 751.

[65] S.O. Rice, Mathematical analysis of random noise, in: N. Wax (Ed.), Selected Papers on Noise and Stochastic Processes, Dover, New York, 1954, p. 133.

[66] H. Risken, The Fokker–Planck Equation, 2nd Ed., Springer, Berlin, 1989.

[67] M.G. Rosenblum, A.S. Pikovsky, J. Kurths, Phase synchronization of chaotic oscillators, Phys. Rev. Lett. 76 (1996) 1804.

[68] M.G. Rosenblum, A.S. Pikovsky, C. Schäfer, P. Tass, J. Kurths, Phase synchronization: from theory to data analysis, in: F. Moss, S. Gielen (Eds.), Neuroinformatics, Handbook of Biological Physics, vol. 4, Elsevier, Amsterdam, 2001, p. 279.

[69] D.F. Russell, L. Wilkens, F. Moss, Use of behavioral stochastic resonance by paddlefish for feeding, Nature 402 (1999) 219.

[70] J.P. Segundo, J.-F. Vibert, K. Pakdaman, M. Stiber, O. Diez Martìnes, Noise and the neurosciences: A long history, a recent revival and some theory, in: K. Pribram (Ed.), Origins: Brain and Self Organization, Lawrence Erlbaum, Hillsdale, NJ, 1994.

[71] E. Simonotto, M. Riani, C. Seife, M. Roberts, J. Twitty, F. Moss, Visual perception of stochastic resonance, Phys. Rev. Lett. 78 (1997) 1186.
[72] E. Simonotto, F. Spano, M. Riani, A. Ferrari, F. Levrero, A. Pillot, P. Renzetti, R. Parodi, F. Sardanelli, P. Vitali, J. Twitty, F. Chiou-Tan, F. Moss, fMRI studies of visual cortical activity during noise stimulation, Neurocomputing 26–27 (1999) 511.
[73] R.L. Stratonovich, in: Topics in the Theory of Random Noise, vol. 2, Gordon and Breach, New York, 1967.
[74] B. Suki, A. Alencar, M.K. Sujeer, K.R. Lutchen, J.J. Collins, J.S. Andrade, E.P. Ingenito, S. Zapperi, H.E. Stanley, Life-support system benefits from noise, Nature 393 (1998) 127.
[75] T.M.P. Tran, F. Moss, L.R. Robinson, F.Y. Chiou-Tan, Increased threshold sural amplitude after upper limb isometric contraction in complete paraplegics, Am. J. Phys. Med. Rehabil. 79 (2000) 542.
[76] M. Usher, M. Feingold, Stochastic resonance in the speed of memory retrieval, Biol. Cybern. 83 (2000) L11.
[77] K. Wiese, Mechanoreceptors for near-field water displacements in crayfish, J. Neurophysiol. 39 (4) (1976) 816.
[78] K. Wiese, R.L. Calabrese, D. Kennedy, Integration of directional mechanosensory input by crayfish interneurons, J. Neurophysiol. 39 (4) (1976) 834.
[79] K. Wiesenfeld, F. Moss, Stochastic resonance and the benefits of noise: from the ice ages to crayfish and squids, Nature 373 (1995) 33.
[80] L.M. Ward, The psychophysics of stochastic resonance, in: P. Killeen (Ed.), Fechner Day 99, International Society for Psychophysics, Tempe, AZ, 1999, p. 389.
[81] L.M. Ward, Dynamical Cognitive Science, MIT, Cambridge, 2002 (Chapter 20–22).
[82] L. Ward, M.S. Desai, D. Rootman, M. Tata, F. Moss, Noise can help as well as hinder seeing and hearing, Bull. Am. Phys. Soc. 46, N23.002 full paper at site: http://www.aps.org/meet/MAR01/baps/vpr/layn23-002.html.
[83] L.M. Ward, A. Neiman, F. Moss, Stochastic resonance in psychophysics and animal behavior, Biol. Cybern. 87 (2002) 91.
[84] P.W. Webb, Kinematics of plaice, *Pleuronectes platessa*, and cod, *Gadus porhua*, swimming near the bottom, J. Exp. Biol. 205 (14) (2002) 2125.
[85] L.A. Wilkens, The crayfish caudal photoreceptor: Advances and questions after the first half century, Comp. Biochem. Physiol. 91 (1988) 61.
[86] L.A. Wilkens, J.K. Douglass, A stimulus paradigm for analysis of near-field hydrodynamics sensitivity in crustaceans, J. Exp. Biol. 189 (1994) 263.
[87] Y. Yamamoto, I. Hidaka, N. Iso-o, A. Komai, R. Soma, S. Kwak, Noise-induced compensation for postural hypotension in primary autonomic failure, Brain Res. 945 (2002) 71.
[88] Y. Yamamoto, I. Hidaka, D. Nozaki, N. Iso-o, R. Soma, S. Kwak, Noise-induced sensitization of human brain, Physica A 314 (2002) 53.
[89] R. Zelick, P.M. Narins, Temporary threshold shift, adaptation, and recovery characteristics of frog auditory nerve fibers, Hear Res. 17 (2) (1985) 161.
[90] P.M. Narins, I. Wagner, Noise susceptibility and immunity of phase locking in amphibian auditory-nerve fibers, J. Acoust. Soc. Am. 85 (3) (1989) 1255.